中國機械工程學刊第四十二卷第一期第 101~111 頁(民國一百一十年)
Journal of the Chinese Society of Mechanical Engineers, Vol.42, No.1, pp 101~111 (2021)

Mathematical Modelling and Experimental Validation of Solar Photovoltaic Thermal (PV/T) Hybrid Air Collector System

R. Senthil Kumar*, E. Natarajan** and N. Puja Priyadharshini***

Keywords：Solar PV/T, Mathematical modelling, Thermal efficiency, Electrical parameter, Parametric analysis

ABSTRACT

In this paper, a steady state one-dimensional mathematical model was developed to analyze the electrical and thermal performance of solar photovoltaic thermal air collector. Comprehensive layer-by-layer mathematical expressions are developed for the temperatures of glass, EVA, PV cell, tedlar of the module, flowing air in the duct, back insulation and useful electrical and thermal energy extraction from solar photovoltaic thermal air collector. An improved correlation is used for calculating the various temperatures, heat transfer coefficients and electrical parameters. Simulated mathematical model results have been compared with the experimental results, and it can be observed a good agreement. Concisely, it is found that the solar photovoltaic thermal system of area 1.5×0.66 m^2 delivers a maximum electrical and thermal efficiency of 14.66% at 16 hr and 26.11% at 12 hr respectively.

INTRODUCTION

Solar photovoltaic thermal (PV/T) systems that convert solar irradiation into electrical and thermal energy. These types of systems incorporate photovoltaic cells, which converts the incident solar radiation into electrical power, with a thermal absorber, which captures the unwanted heat energy and expels waste heat from the PV module.

The utilisation of both electricity and heat permits these systems to have higher energy and consequently higher efficient than solar photovoltaic (PV) system. The increase in solar radiation and ambient temperature increase the PV cell operating temperature considerably, and it significantly reduces the cell efficiency and its life. By cooling the PV module using air or water, the electrical efficiency and life of the PV module can be improved and at the same time, the heat absorbed by the fluid can be used for room heating or warm water applications. Garg and Adhikari (1997) have developed a mathematical model for hybrid photovoltaic thermal air heating system for single and double glass modes. They described the efficiency of the system increases with increase in mass flow rate, length of collector and density of PV cell density and efficiency decreases with increase in the duct depth for both the modes.

Hegazy (2000) examined theoretically the performance of photovoltaic/thermal solar air collector under four modes viz. Mode 1 and 2 (air flows above and below the absorber), Mode 3 and 4 (air flows on both sides as single and double pass). His result shows Mode 3 has highest overall performance and also consumes less fan power. Mode 1 has the lowest overall performance. Tiwari and Sodha (2006) have validated the theoretical model with experimental results for PV/T air-based system and concluded the forced air blowing at the bottom of the PV module increases the overall thermal efficiency by 18%.

Dubey et al. (2009) formulated an analytical model for PV/T hybrid air collector system to predict the electrical efficiency for the glass to tedlar and glass to glass system. He concluded glass to glass with duct PV module gives the higher electrical efficiency of 10.41%. Joshi et al. (2009) have developed a thermal model for integrated PV module and air collector system and validated it experimentally. They reported that the air flow rate decreases the temperature of the PV module and it increases the efficiency of PV module. Solanki et al. (2009) analysed, the indoor PV/T solar heater system under different operating conditions by varying the flow rate of air and solar intensity. They found the

Paper Received September, 2018. Revised November, 2019. Accepted December, 2019. Author for Correspondence: R. Senthil Kumar

* *Associate Professor, Department of Mechanical Engineering, S.A. Engineering College, Chennai 600077, India.*

** *Professor, Department of Mechanical Engineering, Anna University, Chennai 600025, India.*

*** *Graduate Student, Department of Mechanical Engineering,*

thermal and efficiency of the PV/T system was 42% and 8.4% respectively. Agrawal and Tiwari (2010) experimentally investigated the BIPVT system under cold climate conditions for optimizing energy and exergy. He reported the BIPVT system delivers the electrical and thermal exergy of 16,209 kWh and 1531 kWh respectively, at 53.7% overall thermal efficiency under an active area of 65 m^2. Sarhaddi et al. (2010) developed an analytical model to estimate the electrical and thermal parameters for PV/T air collector. They found that the overall thermal, thermal electrical efficiencies reached 45%, 17.18% and 10.01% respectively. Kumar and Rosen (2011) investigated the PV/T solar air heater with a dual pass modes and vertical fins are provided in the lower channel. He concluded the PV cell temperature was reduced from 82°C to 66°C due to extended fins and electrical energy increased considerably. Teo et al. (2012) analysed experimentally and theoretically the behaviour of PV module with and without cooling. An array of air ducts with fins attached beneath of the PV panel to enhance the electrical efficiency. They found, cooling the PV module using air maintain the module temperature around 38°C and the electrical efficiency could be around 12.5%.

Amori and Taqui (2012) have developed Matlab simulation program for solar PV thermal air collector to evaluate the thermal and electrical parameters for summer and winter climate conditions. They have found that the overall thermal efficiency and overall heat loss coefficient are 53.6%, 47.8%, 17.34 W/m^2K, 14.59 W/m^2K for winter and summer conditions respectively. Bahaidarah et. al (2013) analysed the performance of solar photovoltaic module by back surface water cooling and found the module temperature decreased about 20% and PV panel electrical efficiency increased by 9%. Abu Bakar et. al (2014) developed a 2D energy balance equations for bi-fluid PV/T solar collector to estimate the electrical efficiency and the temperatures of PV cell, tedlar, rear panel and both fluids. He concluded at the optimum mass flow rate of 0.041 kg/s the electrical efficiency increases up to 10.7%. Kessaissia et. al (2015) developed implicit and explicit mathematical model for polycrystalline and monocrystalline silicon module to estimate the I-V characteristics of the PV module and validated with experimental results. He concluded that the implicit model gives more accurate results than the explicit model.

So far, no detailed mathematical model is available to predict the temperature on each layer of the PV/T system. The primary objective of the present mathematical modelling is to determine the temperature of each layer of PV/T system viz., glass top, top EVA, PV cell, bottom EVA, tedlar, insulation inside, insulation outside and an outlet air. Based on temperature, the electrical and thermal performance of PV/T system are computed. Detailed steady state equations for the solar PV/T system operating under bottom forced air-cooling mode is presented. Improved correlation is used for calculating the sky temperature, Nusselt number, radiation and wind heat transfer coefficient. An enhanced five parameter electrical model will be used to assess the electrical parameters of solar photovoltaic module such as V_{oc}, I_{sc}, V_{mp}, I_{mp}, and P_{mp}. The electrical and thermal performance of the system have been analysed. An experimental study was initiated to validate the present mathematical model results.

ANALYTICAL MODELLING

The PV/T system shown in Fig. 1, consists of a glass cover, top EVA, PV cell layer, bottom EVA, tedlar, air flow duct and bottom insulation. The various layer temperatures, PV module electrical parameters, thermal, electrical and overall efficiency of the PV/T system are evaluated by the use of thermal and electrical modelling. The various design parameters of the PV/T air collector system used in this study are given in Table 1.

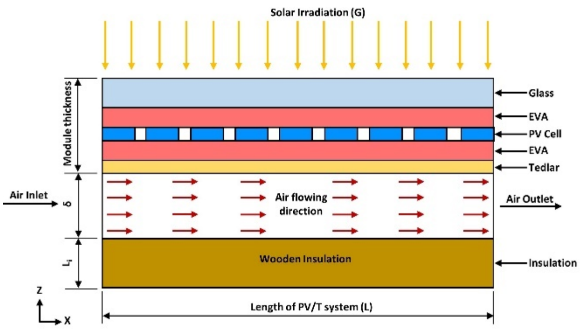

Fig. 1. Schematic cross-sectional diagram of solar PV/T system.

Table 1. Design parameters used in the present PV/T modelling.

Parameter	Value	Parameter	Value
L	1.5 m	k_g	2 W/mK
B	0.66 m	k_e	0.311 W/mK
δ	0.03 m	k_c	130 W/mK
C_f	0.36	k_t	0.15 W/mK
α_g	0.04	k_i	0.035 W/mK
α_e	0.08	L_g	0.003 m
α_c	0.9	L_e	0.0005 m
α_t	0.128	L_c	0.0002 m
τ_g	0.92	L_t	0.0003 m
τ_e	0.9	L_i	0.05 m
τ_c	0.02	V_w	1.5 m/s
τ_t	0.012	σ	5.669×10^{-8} W/m^2K^4
ε_g	0.85	G_{ref}	1000 W/m^2
ε_t	0.9	$E_{g,ref}$	1.794×10^{-19} J
ε_i	0.86	K	1.381×10^{-23} J/K
β_c	0.83	C	0.0002677 K^{-1}

Thermal modelling

The one-dimensional steady state condition considered for the mathematical formulation in the flow direction. Also, the energy balance equations for various layers of the solar PV/T system are written by considering the following simplifying assumptions: The air leakage of the PV/T system and the edge losses are negligible. The duct air temperature varies only in the flow direction. All the materials used in the mathematical model is isotropic and independent of the temperature. The heat transfer in electrical busbar and fingers of the solar panel are neglected in the mathematical model for simplicity. All the side walls of the PV/T system are taken to be adiabatic. The ambient temperature is same on all area exposed to the environment. The reference temperature and pressure are 25°C and 101325 Pa. Solar radiation is not reflected on any surface and is fully transmitted to the layer below. The flow is steady, turbulent and one-dimensional. The steady state conditions are performed.

According to considered assumptions and thermal network diagram presented in Fig. 2, the energy balance equations for various layers of the solar PV/T system can be expressed as follows:

For glass top

[The rate of solar energy available on glass] + [Conductive heat transfer from EVA-1 to the glass] = [Convective heat loss from glass to ambient] + [Radiative heat loss from glass to ambient]

$$\alpha_g G + U_g\left(T_{e,1} - T_g\right) = h_w\left(T_g - T_a\right) + h_{r,g-s}\left(T_g - T_{sky}\right) \quad (1)$$

Where G, α_g, U_g, h_w, $h_{r,g-s}$, T_{sky}, T_a, T_g and $T_{e,1}$ are incident solar radiation, absorptivity of glass, conductive heat transfer coefficient between glass and upper EVA, convective heat transfer coefficient between glass top and ambient air, radiative heat transfer between glass top and sky, sky temperature, ambient temperature, glass temperature and upper EVA temperature respectively.

For EVA-1 (Upper EVA)

[The rate of solar energy available on upper EVA] + [Conductive heat transfer from PV cells to upper EVA] = [Conductive heat transfer from upper EVA to the glass]

$$\alpha_e \tau_g G + U_e \beta_c\left(T_c - T_{e,1}\right) = U_g\left(T_{e,1} - T_g\right) \quad (2)$$

Where, α_e, τ_g, U_e, β_c and T_c are absorptivity of EVA, transmissivity of glass, conductive heat transfer coefficient between PV cell and upper EVA, packing factor of solar cells and PV cell temperature respectively.

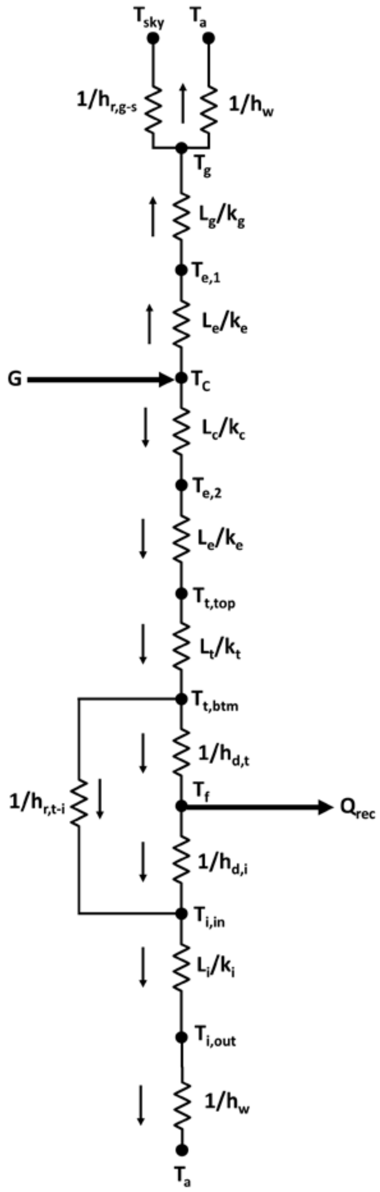

Fig. 2. Thermal network diagram of PV/T system.

For PV cell

[The rate of solar energy available on PV cells] = [Rate of electrical power produced] + [Conductive heat transfer from PV cells to upper EVA] + [Conductive heat transfer from PV cells to lower EVA]

$$\alpha_c \tau_e \tau_g \beta_c G = E_p + U_e \beta_c\left(T_c - T_{e,1}\right) + U_c \beta_c\left(T_c - T_{e,2}\right) \quad (3)$$

Where, α_c, τ_e, E_p, U_c and $T_{e,2}$ are the absorptivity of PV cell, the transmissivity of upper EVA, electrical power generation of PV module, conductive heat transfer coefficient between PV cell and lower EVA and temperature of lower EVA.

For EVA-2 (Lower EVA)
[The rate of solar energy available on lower EVA] + [Conductive heat transfer from PV cells to lower EVA] = [Conductive heat transfer from lower EVA to tedlar]

$$\left[\alpha_e\tau_c\tau_e\tau_g\beta_c G+\left(1-\beta_c\right)\alpha_e\tau_e\tau_g G\right] + U_c\beta_c\left(T_c-T_{e,2}\right)=U_e\left(T_{e,2}-T_{t,top}\right) \quad (4)$$

Where, U_e and $T_{t,top}$ are conductive heat transfer coefficient between lower EVA and tedlar top and temperature of the inner surface of the tedlar.

For tedlar top side
[The rate of solar energy available on tedlar] + [Conductive heat transfer from lower EVA to tedlar top] = [Conductive heat transfer from tedlar top to tedlar bottom]

$$\left[\alpha_t\tau_c\tau_e^2\tau_g\beta_c G+\left(1-\beta_c\right)\alpha_t\tau_e^2\tau_g G\right] + U_e\left(T_{e,2}-T_{t,top}\right)=U_t\left(T_{t,top}-T_{t,btm}\right) \quad (5)$$

For tedlar bottom side
[Conductive heat transfer from tedlar top to tedlar bottom] = [Convective heat transfer from tedlar bottom to flowing air] + [Radiative heat transfer from tedlar bottom to insulation inside]

$$U_t\left(T_{t,top}-T_{t,btm}\right)=h_{d,t}\left(T_{t,btm}-T_f\right) + h_{r,t-i}\left(T_{t,btm}-T_{i,in}\right) \quad (6)$$

For air medium
Referring Fig. 2 the energy balance equation for an element (dx) of flowing air in the duct can be written as:
[Convective heat transfer from tedlar bottom to flowing air] = [Rate of heat gain by the flowing air] + [Convective heat transfer from flowing air to insulation inside]

$$h_{d,t}\left(T_{t,btm}-T_f\right)Bdx=\dot{m}C_p\left(\frac{dT_f}{dx}\right)dx + h_{d,i}\left(T_f-T_{i,in}\right)Bdx \quad (7)$$

For insulation inside
[Convective heat transfer from flowing air to insulation inside] + [Radiative heat transfer from tedlar bottom to insulation inside] = [Conductive heat transfer from insulation inside to insulation outside]

$$h_{d,i}\left(T_f-T_{i,in}\right)+h_{r,t-i}\left(T_{t,btm}-T_{i,in}\right) =U_i\left(T_{i,in}-T_{i,out}\right) \quad (8)$$

For insulation outside
[Conductive heat transfer from insulation inside to insulation outside] = [Convective heat transfer from insulation outside to ambient air]

$$U_i\left(T_{i,in}-T_{i,out}\right)=h_w\left(T_{i,out}-T_a\right) \quad (9)$$

Dimensionless numbers and heat transfer coefficients

The convection heat transfer coefficient depends on the physical configuration and also various properties of the agent fluid (air) used. Empirical correlations are available to evaluate the heat transfer coefficients for several forced convection heat transfer configurations. Those correlations are usually expressed in terms of dimensionless numbers. The dimensionless numbers used for forced convection heat transfer coefficients are the Nusselt number (Nu), Prandtl number (Pr), and Reynolds number (Re). The heat transfer coefficient (h), computed from Nusselt number. Hence those correlations are typically in the form of an equation for Nu in relation with Re and Pr.

The Reynolds number for rectangular air duct in PV/T system is:

$$R_e=\frac{\rho v D_h}{\mu_f} \quad (10)$$

'v' is velocity in the air duct is:

$$v=\frac{\dot{m}}{\rho B\delta} \quad (11)$$

D_h is equivalent diameter for the simple rectangular air duct is:

$$D_h=\frac{2\delta B}{\left(\delta+B\right)} \quad (12)$$

The Prandtl number for simple rectangular air duct in PV/T system is:

$$Pr=\frac{\mu_f C_p}{k_{air}} \quad (13)$$

The Nusselt number for turbulent flow inside a simple rectangular air duct in PV/T system is estimated using Dittus and Boelter equation in Holman (2010):

$$Nu=0.023\left(Re\right)^{0.8}\left(Pr\right)^{0.4} \quad (14)$$

To estimate the density, thermal conductivity, and dynamic viscosity of flowing air in duct can be obtained as Mohammadi (2013):

$$\rho_{air} = 3.9147 - 0.016083T_a + 2.9013\times10^{-5}T_a^2 - 1.9407\times10^{-8}T_a^3 \quad (15)$$

$$k_{air} = (0.0015215 + 0.097459T_a - 3.3322\times10^{-5}T_a^2)\times10^{-3} \quad (16)$$

$$\mu_{f-air} = (1.6157 + 0.06523T_a - 3.0297\times10^{-5}T_a^2)\times10^{-6} \quad (17)$$

The convective heat transfer coefficient h_w due to wind flowing over the top surface of the glass and the bottom surface of the insulation recommended by Wattmuff et al. (1977), is calculated from:

$$h_w = 2.8 + 3V_w \quad (18)$$

The heat transfer coefficient due to convection from the tedlar back side to flowing air can be estimated via

$$h_{d,t} = \frac{Nu\ k_{air}}{D_h} \quad (19)$$

The heat transfer coefficient due to convection from the insulation inside to flowing air $h_{d,i}$ which can be estimated similar to $h_{d,t}$. The radiation heat transfer coefficient from the glass top to ambient are:

$$h_{r,g-s} = \varepsilon_g \sigma \frac{(T_g^4 - T_{sky}^4)}{(T_g - T_a)} \quad (20)$$

The effective sky temperature T_{sky} is calculated from the following empirical relation recommended by Duffie and Beckman (2013):

$$T_{sky} = T_a \sqrt[4]{\begin{pmatrix} 0.711 + 0.0056T_{dp} + 0.000073T_{dp}^2 \\ + 0.013\cos(15t) \end{pmatrix}} \quad (21)$$

Where T_{dp} is the dew point temperature in (°C) and 't' is time (hr) from midnight.

The radiation heat transfer coefficient from the tedlar bottom to insulation inside are:

$$h_{r,t-i} = \frac{\sigma\left(T_t + T_{i-in}\right)\left(T_t^2 + T_{i-in}^2\right)}{\dfrac{1}{\varepsilon_t} + \dfrac{1}{\varepsilon_i} - 1} \quad (22)$$

The conductive heat transfer coefficients in Eqs. (1)–(6) are:

$$U_g = k_g / L_g \quad (23)$$

$$U_e = k_e / L_e \quad (24)$$

$$U_c = k_c / L_c \quad (25)$$

$$U_t = k_t / L_t \quad (26)$$

$$U_i = k_i / L_i \quad (27)$$

Where k_g, L_g, k_e, L_e, k_c, L_c, k_t, L_t, k_i and L_i are the corresponding thermal conductivity and thickness of glass, EVA, solar cell, tedlar and insulation material in (W/m^2K) and (m) respectively.

Air flow temperature in duct

An ordinary differential equation (ODE) for the air flow temperature (T_f) inside the duct from equation (7) is given by,

$$\frac{dT_f}{dx} = \frac{B}{\dot{m}C_p}\left[h_{d,t}(T_{t,btm} - T_f) - h_{d,i}(T_f - T_{i,in})\right] \quad (28)$$

The expression for air flow temperature inside the rectangular duct can be obtained by integrating Eq. (28) with the following boundary conditions is given by,

$$BC:\ T_f = T_{f,in},\ at\ x = 0$$

$$T_f(x) = \left\{\left(1 - exp\left(\frac{-\left(h_{d,t} + h_{d,i}\right)Bx}{\dot{m}C_p}\right)\right)\left(\frac{h_{d,i}T_{i,in} + h_{d,t}T_{t,btm}}{h_{d,t} + h_{d,i}}\right)\right\} + T_{f,in}exp\left(\frac{-\left(h_{d,t} + h_{d,i}\right)Bx}{\dot{m}C_p}\right) \quad (29)$$

The expression for outlet air temperature of the flowing air can be obtained by substituting the following boundary conditions in Eq. (29) is given by,

$$BC:\ T_f = T_{f,out},\ at\ x = L$$

$$T_{f,out} = \left\{\left(1 - exp\left(\frac{-\left(h_{d,t} + h_{d,i}\right)BL}{\dot{m}C_p}\right)\right)\left(\frac{h_{d,i}T_{i,in} + h_{d,t}T_{t,btm}}{h_{d,t} + h_{d,i}}\right)\right\} + T_{f,in}exp\left(\frac{-\left(h_{d,t} + h_{d,i}\right)BL}{\dot{m}C_p}\right) \quad (30)$$

The expression for average air flow temperature $\overline{T_f}$ over the full length of air duct is given by,

$$\overline{T_f} = \frac{1}{L}\int_{x=0}^{L} T_f(x)\,dx \quad (31)$$

$$\overline{T_f} = \frac{\left\{ \left(\frac{BL\left(h_{d,t}+h_{d,i}\right)}{\dot{m}C_p} exp\left(\frac{BL\left(h_{d,t}+h_{d,i}\right)}{\dot{m}C_p} \right) + 1 \right) \left(\frac{h_{d,i}T_{i,in} + h_{d,t}T_{t,btm}}{h_{d,t}+h_{d,i}} \right) \right\} - T_{f,in}}{\frac{BL\left(h_{d,t}+h_{d,i}\right)}{\dot{m}C_p} exp\left(\frac{BL\left(h_{d,t}+h_{d,i}\right)}{\dot{m}C_p} \right)} - \frac{\dot{m}C_p\left(\left(h_{d,i}T_{i,in} + h_{d,t}T_{t,btm} \right) - T_{f,in}\left(h_{d,t}+h_{d,i}\right) \right)}{BL\left(h_{d,t}+h_{d,i}\right)} \quad (32)$$

Electrical modelling

The thermal and electrical model are dependent on each other. To solve the thermal model, we need electrical efficiency. In the earlier studies, the electrical efficiency of a PV module has been evaluated by using Eq. (33).

$$\eta_{ele} = \eta_{ele,ref}\left[1 - 0.0045\left(T_c - T_a\right)\right] \quad (33)$$

The Eq. (33) has some deficiencies as pointed below:

- At low solar radiation, the PV module electrical efficiency equals to the reference electrical efficiency $\left(\eta_{ele} \approx \eta_{ele,ref} = 0.15\right)$.
- The temperature difference between solar cell and ambient is very less is the reason for this fact.
- It cannot calculate the electrical parameters of PV module such as V_{oc}, I_{sc}, V_{mp}, I_{mp} and P_{mp}.

In the present mathematical model, the electrical efficiency and electrical parameters of PV module are computed by use of the five parameters electrical model. The Fig. 3 and Fig. 4 shows the one diode electrical equivalent circuit and I-V characteristics of PV module given by Boyle (2004) respectively. The characteristics equation of single diode five parameter model of PV module is recommended by Duffie and Beckman (2013) is defined as:

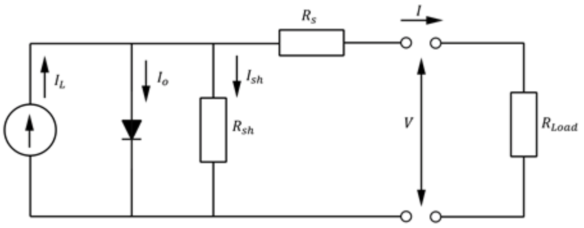

Fig. 3. 5-parameter equivalent circuit of a PV module.

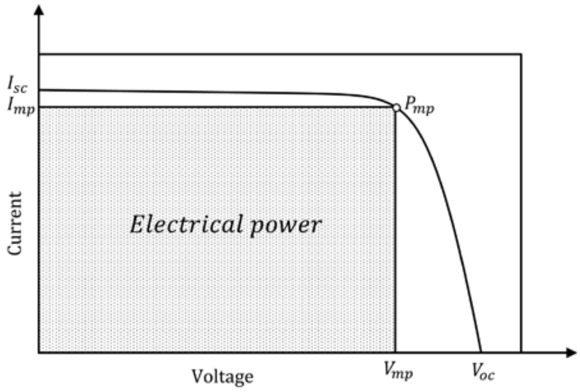

Fig. 4. PV module current-voltage (I-V) characteristics curve.

$$I = I_L - I_o\left[exp\left(\frac{V+IR_s}{a}\right) - 1\right] - \frac{V+IR_s}{R_{sh}} \quad (34)$$

The five parameters in the above equation (34) are light current (I_L), diode reverse saturation current (I_o), series resistance (R_s), shunt resistance (R_{sh}), and ideality factor (a). These five parameters are to be first found at reference conditions (G_{ref} = 1000 W/m^2, and $T_{cell,ref}$ = 25°C) then they are to be translated to the any required operating conditions. In order to calculate five reference parameters ($I_{L,ref}$, $I_{o,ref}$, $R_{s,ref}$, $R_{sh,ref}$ and a_{ref}), five equations are needed at reference conditions. In general, the manufacture of PV module provides open circuit voltage, short circuit current, maximum power voltage, maximum power current, current temperature coefficient and voltage temperature coefficient. From literature, author found that the ideality factor (a) for PV module is vary in between 0 to 3. In this paper, the author iteratively varies the ideality factor in between 0 and 3 with a step size of 10^{-3} and simultaneously solve the equations (35)–(38) till it reaches the given manufacturer reference maximum power with minimal relative error. Hence four equations are enough to find the remaining reference parameters. These four equations are obtained by substituting the following four conditions in equation (34).

At short circuit current: $I = I_{sc,ref}$, $V = 0$.

At open circuit voltage: $I = 0$, $V = V_{oc,ref}$.

At maximum power point: $I = I_{mp,ref}, V = V_{mp,ref}$.

At maximum power point: $\left[\frac{d(IV)}{dV}\right]_{mp} = \left[\frac{dP}{dV}\right]_{mp} = 0$

Substituting the above four conditions into equation (34), the following equations are obtained.

$$I_{sc,ref} = I_{L,ref} - I_{o,ref}\left[exp\left(\frac{I_{sc,ref}R_{s,ref}}{a_{ref}}\right)-1\right] - \frac{I_{sc,ref}R_{s,ref}}{R_{sh,ref}} \quad (35)$$

$$0 = I_{L,ref} - I_{o,ref}\left[exp\left(\frac{V_{oc,ref}}{a_{ref}}\right)-1\right] - \frac{V_{oc,ref}}{R_{sh,ref}} \quad (36)$$

$$I_{mp,ref} = I_{L,ref} - \left[\frac{V_{mp,ref}+I_{mp,ref}R_{s,ref}}{R_{sh,ref}}\right] - I_{o,ref}\left[exp\left(\frac{V_{mp,ref}+I_{mp,ref}R_{s,ref}}{a_{ref}}\right)-1\right] \quad (37)$$

$$\frac{I_{mp,ref}}{V_{mp,ref}} = \frac{\left\{\left(\frac{I_{o,ref}}{a_{ref}}\right) exp\left(\frac{V_{mp,ref}+I_{mp,ref}R_{s,ref}}{a_{ref}}\right)\right\} + \frac{1}{R_{sh,ref}}}{1+\frac{R_{s,ref}}{R_{sh,ref}}+\left\{\left(\frac{I_{o,ref}R_{s,ref}}{a_{ref}}\right) exp\left(\frac{V_{mp,ref}+I_{mp,ref}R_{s,ref}}{a_{ref}}\right)\right\}} \quad (38)$$

To calculate the PV module five parameters at operating conditions (G_{new} and $T_{c,new}$), the following equations are used

$$\frac{a_{new}}{a_{ref}} = \frac{T_{c,new}}{T_{c,ref}} \quad (39)$$

$$I_{L,new} = \left(\frac{G_{new}}{G_{ref}}\right)\left[I_{L,ref}+\alpha\left(T_{c,new}-T_{c,ref}\right)\right] \quad (40)$$

$$\frac{I_{o,new}}{I_{o,ref}} = \left(\frac{T_{c,new}}{T_{c,ref}}\right)^3 exp\left[\frac{1}{K}\left(\frac{E_{g,ref}}{T_{c,ref}}-\frac{E_{g,new}}{T_{c,new}}\right)\right] \quad (41)$$

$$\frac{E_{g,new}}{E_{g,ref}} = 1 - C\left(T_{c,new}-T_{c,ref}\right) \quad (42)$$

$$\frac{R_{sh,new}}{R_{sh,ref}} = \frac{G_{ref}}{G_{new}} \quad (43)$$

$$R_{s,new} = R_{s,ref} \quad (44)$$

Where E_g, K and C are the silicon band gap energy, Boltzmann's constant and the temperature coefficient for bandgap energy respectively.

Utilizing the five electrical parameters for operating conditions calculated above, the V_{mp}, I_{mp}, V_{oc} and I_{sc} at operating conditions are obtained by simultaneously solving the Eqs. (45) – (48).

$$V_{mp,new} = \frac{I_{mp,new}\left[1+\frac{R_{s,new}}{R_{sh,new}}+\left(\frac{I_{o,new}R_{s,new}}{a_{new}}\right)\exp\left(\frac{V_{mp,new}+I_{mp,new}R_{s,new}}{a_{new}}\right)\right]}{\left\{\frac{I_{o,new}}{a_{new}}\exp\left(\frac{V_{mp,new}+I_{mp,new}R_{s,new}}{a_{new}}\right)\right\}+\frac{1}{R_{sh,new}}} \quad (45)$$

$$I_{mp,new} = I_{L,new} - \left[\frac{V_{mp,new}+I_{mp,new}R_{s,new}}{R_{sh,new}}\right] - I_{o,new}\left[exp\left(\frac{V_{mp,new}+I_{mp,new}R_{s,new}}{a_{new}}\right)-1\right] \quad (46)$$

$$V_{oc,new} = R_{sh,new}\left[I_{L,new} - I_{o,new}\left[exp\left(\frac{V_{oc,new}}{a_{new}}\right)-1\right]\right] \quad (47)$$

$$I_{sc,new} = I_{L,new} - I_{o,new}\left[exp\left(\frac{I_{sc,new}R_{s,new}}{a_{new}}\right)-1\right] - \frac{I_{sc,new}R_{s,new}}{R_{sh,new}} \quad (48)$$

The maximum power of PV module at operating conditions is given by:

$$P_{mp,new} = V_{mp,new}I_{mp,new} \quad (49)$$

The fill factor FF is the ratio of maximum power (P_{mp}) to the product of open circuit voltage (V_{oc}) and the short circuit current (I_{sc}). This factor is calculated as:

$$FF = \frac{P_{mp}}{V_{oc}I_{sc}} \quad (50)$$

Efficiency calculation

The thermal efficiency of the PV/T air collector is defined as:

$$\eta_{th} = \frac{\dot{Q}_{rec}}{BLG} \quad (51)$$

The electrical efficiency of the PV module at operating conditions is calculated as:

$$\eta_{ele} = \frac{P_{mp,new}}{G_{new}A_{mod}} \quad (52)$$

The thermal equivalent electrical efficiency is defined as:

$$\eta_{ele,th} = \frac{\eta_{ele}}{C_f} \tag{53}$$

Where $C_f = 0.36$ is the thermal power plant conversion factor for India.

The overall thermal energy of a PV/T air collector is given by:

$$\eta_{th,ovl} = \eta_{th} + \eta_{ele,th} = \eta_{th} + \frac{\eta_{ele}}{C_f} \tag{54}$$

EXPERIMENTAL ANALYSIS

Experimental PV/T system description

A polycrystalline silicon PV module is mounted on a rectangular wooden duct and the PV/T system mounted on a rigid steel frame for the stability of the system and ease of inclination angle adjustment. Hard plywood was used for making air duct. The side gaps of the PV/T system are fully sealed to prevent the air leakage. A small air blower is used to force the air through the duct. The mass flow rate of air was controlled by a valve placed in between blower and inlet of PV module. The specification of the PV module used in this study are given in Table 2.

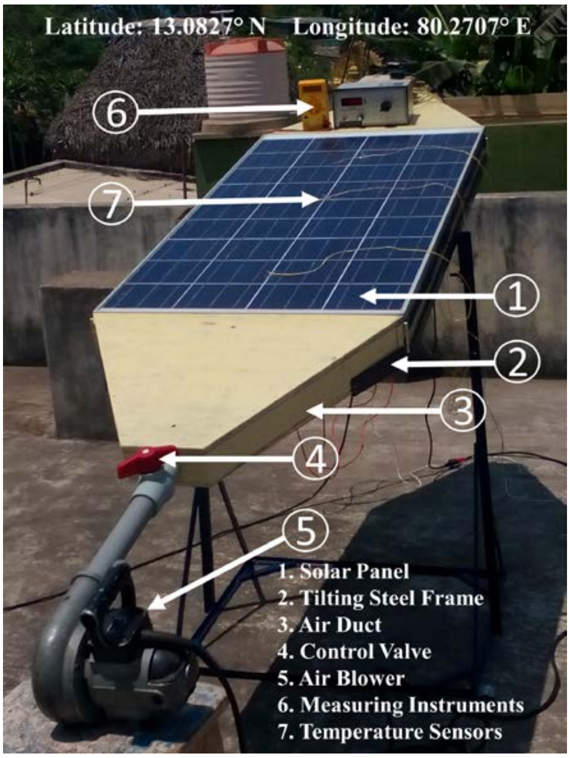

Fig. 5. Experimental setup of solar PV/T system.

The outdoor experiment was conducted in Institute for Energy Studies, Anna University, Chennai, India (13.0827° N, 80.2707° E) and the experiment rig with air cooling is shown in Fig. 5. The experiment was conducted from 8.00 am to 4.00 pm on a clear sunny days. Experiment tests was performed for PV module without cooling (WOC) and PV module with air cooling (WAC) simultaneously. The optimum tilt angle of the PV module during the test period is set as 13° facing towards South. The solar radiation is measured by digital solarimeter installed parallel to the PV module plane. A well-calibrated k-type thermocouple are used to measure the various temperature of the PV/T system such as top glass, PV cell, tedlar bottom, insulation inside, insulation outside, ambient, inlet air and outlet air. The wind velocity and air velocity in the duct have been measured with the help of an anemometer. Digital multimeter (DMM) has been used to measure the current and voltage of the PV module. All the experimental parameters are measured on an hourly basis.

Table 2. Specifications of PV module.

Name	Value
Peak Power, P_{mp}	150 W
Rated Voltage, V_{mp}	17.84 V
Rated Current, I_{mp}	8.4 A
Open Circuit Voltage, V_{oc}	22.35 V
Short Circuit Current, I_{sc}	8.9 A

RESULTS AND DISCUSSION

Experimental validation

The present mathematical model results have been validated by their corresponding experimental values. The root mean square percentage error (RMSE) and R-squared values are calculated by comparing the simulated results with experimental results using Eqs. (55) and (56) recommended by Dubey et al. (2009). It is clear from the errors that the present mathematical model results are in good agreement with the experimental results.

$$RMSE = \sqrt{\frac{\sum \left(100 \times (X_i - Y_i) / X_i\right)^2}{m}} \tag{55}$$

$$R^2 = \frac{\left[m\left(\sum_{i=1}^{m} X_i Y_i\right) - \left(\sum_{i=1}^{m} X_i\right)\left(\sum_{i=1}^{m} Y_i\right)\right]^2}{\left[m\sum_{i=1}^{m} X_i^2 - \left(\sum_{i=1}^{m} X_i\right)^2\right]\left[m\sum_{i=1}^{m} Y_i^2 - \left(\sum_{i=1}^{m} Y_i\right)^2\right]} \tag{56}$$

Where, X_i is the ith simulated value, Y_i is the ith experimental value and 'm' is the number of data points.

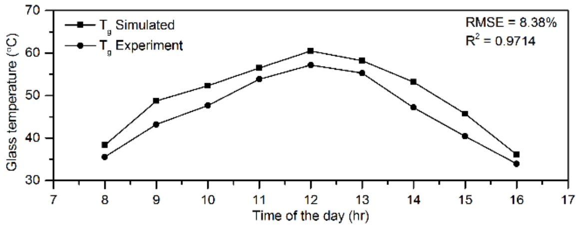

Fig. 6. Glass temperature.

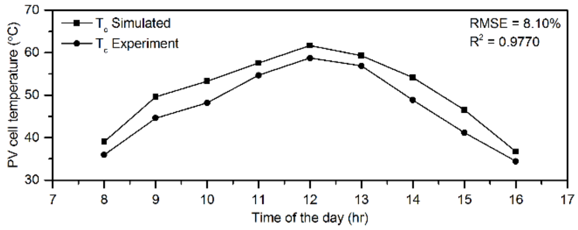

Fig. 7. PV cell temperature.

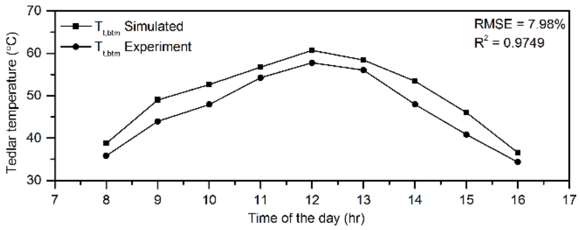

Fig. 8. Tedlar temperature.

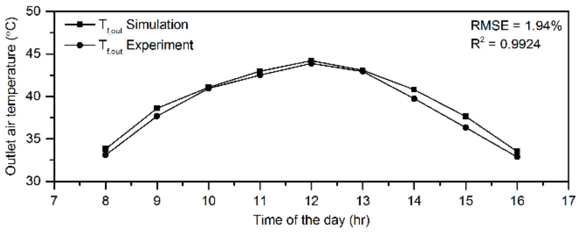

Fig. 9. Outlet air temperature.

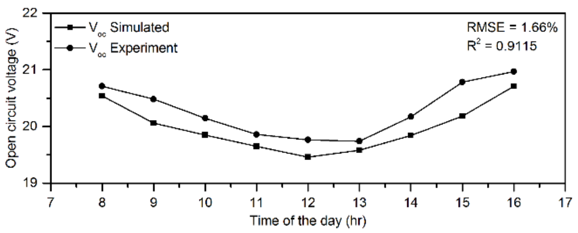

Fig. 10. Open circuit voltage.

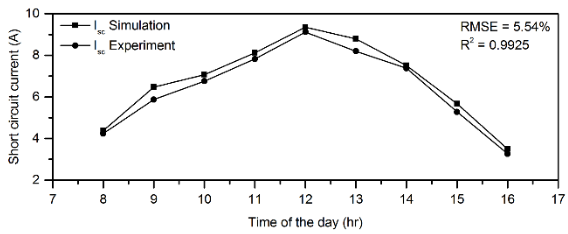

Fig. 11. Short circuit current.

The simulated values are compared with the experimental values during the test day, and proportionate error values are generated are given in Table 3. Fig. 6 shows the hourly deviation of simulated and experimental values of glass temperature for solar PV/T air collector system. The root mean square percentage error (RMSE) and R-squared value (R^2) for glass temperature are found to be 8.38% and 0.9714 respectively. The simulated and experimental values of PV cell, tedlar and outlet air temperature are shown in Fig. 7, 8 and 9 respectively. The RMSE of these parameters are 8.10%, 7.98% and 1.94% respectively with the corresponding R^2 as 0.9770, 0.9749 and 0.9924 respectively. It is observed that the simulated values of the thermal model are good agreement with the experimental results. The simulated and experimental values of V_{oc} are shown in Fig. 10. The values of RMSE and R^2 are found to be 1.66% and 0.9115 respectively. The Fig. 11 shows the simulated and experimental values of I_{sc} during the experiment day. The RMSE and R-squared values are 5.54% and 0.9925 respectively. It can be observed that the simulated values of present five parameters electrical model are in good conformity with the experimental results.

Table 3. RMSE and R^2 values.

Name	RMSE (%)	R^2
T_g	8.38	0.9714
T_c	8.10	0.9770
T_t	7.98	0.9749
$T_{f,out}$	1.94	0.9924
V_{oc}	1.66	0.9115
I_{sc}	5.54	0.9925

Based on time of the day

The hourly variants of solar intensity, ambient temperature and sky temperature in the environment conditions of Chennai for a typical sunny day have been shown in Fig. 12. The hourly simulated top glass, PV cell, tedlar bottom, and outlet air temperature on their corresponding ambient temperature are shown in Fig. 13. The outlet air temperature was 33.52°C and 44.22°C at 16 hr and 12 hr respectively and peak simulated cell and glass temperature was found to be 61.67°C and 60.49°C at 12 noon respectively. At 16 hr the simulated tedlar bottom temperature was found to be the minimum value of 36.56°C and at 12 noon it reaches a peak value of 60.71°C.

Due to the wind, more heat transfer occurs on the top side of the PV/T system hence most of the times the glass temperature was less than that of tedlar temperature. The maximum difference between cell temperature and ambient temperature was found to be 24.06°C at 12 noon and the minimum difference was found to be 4.38°C at 16 hr. The simulated values of cell temperature for WAC and

WOC PV module are shown in Fig. 14. The minimum and maximum difference between WAC and WOC PV module cell temperatures are 3.60°C at 16 hr and 8.06°C at 12 noon respectively. The Fig. 15 shows the hourly simulated thermal, electrical, and overall efficiency. The electrical efficiency ranged between 12.65% and 14.66% throughout the day whereas the thermal efficiency varies from 12.18% to 26.11%. The overall efficiency ranged (52.93 – 61.41%).

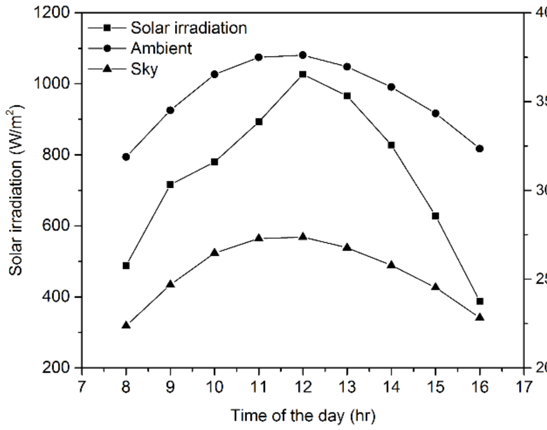

Fig. 12. Hourly variation of G, T_a, and T_{sky}.

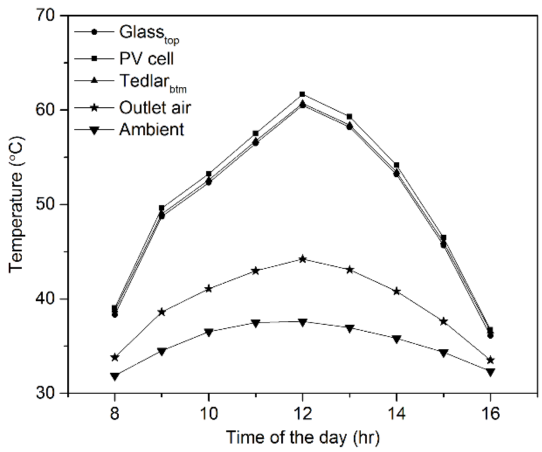

Fig. 13. Hourly variation of simulated T_g, T_c, $T_{t,btm}$, and $T_{f,out}$.

Table 4. Simulation results at 12 noon.

Electrical parameter	Value	Thermal parameter	Value
a	1.022	T_g	60.49 °C
I_L	9.334 A	$T_{e,1}$	61.07 °C
I_o	3.709×10^{-08} A	T_c	61.67 °C
R_s	0.2175 Ω	$T_{e,2}$	61.67 °C
R_{sh}	973.1 Ω	$T_{t,btm}$	60.71 °C
V_{oc}	19.77 V	$T_{f,in}$	37.62 °C
I_{sc}	9.332 A	$T_{f,out}$	44.22 °C
V_{mp}	15.19 V	T_f	41.19 °C
I_{mp}	8.653 A	$T_{i,in}$	48.27 °C
P_{mp}	131.4 W	$T_{i,out}$	38.76 °C
η_{ele}	12.92%	η_{th}	26.11%

From Fig. 15 it is found that the maximum thermal efficiency occurs where the electrical efficiency is minimum and vice versa. Fig. 16 shows the simulated values of maximum power for with and without air cooling of solar panel. The minimum and maximum difference between P_{mp} for WAC and WOC are 0.92 W at 16 hr and 7 W at 12 noon respectively. The consolidated simulated results of electrical and thermal parameters of the present study at 12 noon are given in Table 4.

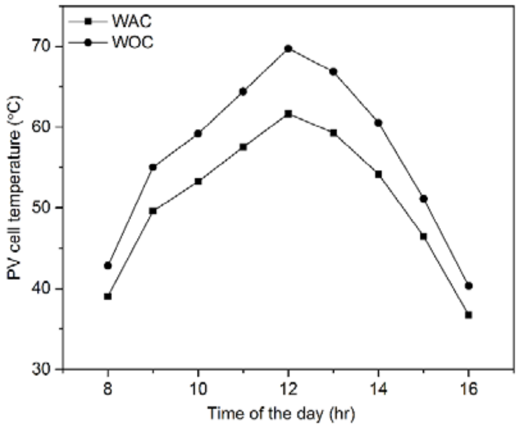

Fig. 14. Hourly variation of simulated Tc.

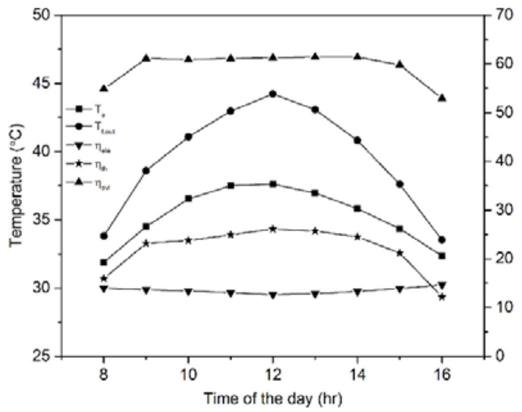

Fig. 15. Hourly variation of simulated η_{th}, η_{el}, and η_{ovl}.

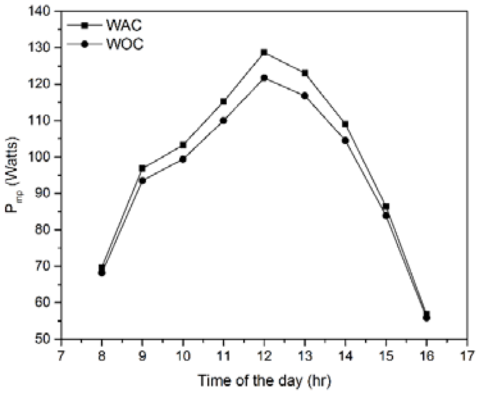

Fig. 16. Hourly variation of simulated P_{mp}.

CONCLUSIONS

In this study, an improved and layer by layer detailed theoretical energy analysis of solar photovoltaic thermal (PV/T) system performance has been carried out. The thermal model used in the present analysis gives more accurate results and also it predicts the temperature of each layer of PV/T system viz., glass top, top EVA, PV cell, bottom EVA, tedlar, insulation inside, insulation outside and an outlet air. The five-parameter electrical model used in this paper gives accurate results and also it predicts the V_{oc}, I_{sc}, V_{mp}, I_{mp} and P_{mp} with greater accuracy. The PV module electrical efficiency is sensitive to the panel temperature and decreases as the temperature of the panel increases. With forced air-cooling technique, the operating temperature of the module is found drop significantly to about 25% and an increase of 10% in the electrical efficiency is observed. On the basis of thermal and electrical efficiency, the thermal efficiency attains a maximum value where the electrical efficiency is minimum and vice versa. The results of the present mathematical model are in good agreement with the present experimental measurements with respect to RMSE percentage and R-squared errors. The working fluid has a great effect on the cell temperature minimization. Air has lower thermal conductivity than other fluids. The electrical efficiency and thermal efficiency can be further increased by providing fin and baffles in the air duct. Otherwise, water or nanofluid is also used in PV/T collector system for a further increase in efficiency of the system.

REFERENCES

Agrawal, B. and Tiwari, G. N., "Optimizing the energy and exergy of building integrated photovoltaic thermal (BIPVT) systems under cold climatic conditions," *Appl. Energy*, Vol. 87, pp. 417–426. (2010).

Amori, K. E. and Taqi, A.-N. H. M., "Analysis of thermal and electrical performance of a hybrid (PV/T) air based solar collector for Iraq," *Appl. Energy*, Vol. 98, pp. 384–395. (2012).

Abu Bakar, M. N., Othman, M., Din, M. H., Manaf, N. A. and Jarimi, H., "Design concept and mathematical model of a bi-fluid photovoltaic/thermal (PV/T) solar collector," *Renew. Energy*, Vol. 67, pp. 153–164. (2014).

Boyle, G., Renewable Energy Power for a Sustainable Future, Oxford University Press, (2004).

Bahaidarah, H., Subhan, A., Gandhidasan, P. and Rehman, S., "Performance evaluation of a PV (photovoltaic) module by back surface water cooling for hot climatic conditions," *Energy*, Vol. 59, pp. 445–453. (2013).

Dubey, S., Sandhu, G. S. and Tiwari, G. N., "Analytical expression for electrical efficiency of PV/T hybrid air collector," *Appl. Energy*, Vol. 86, pp. 697–705. (2009).

Duffie, J. A. and Beckman, W. A., *Solar engineering thermal processes*, John Wiely & Sons Inc., (2013).

Garg, H. P. and Adhikari, R. S., "Conventional hybrid photovotaic/thermal (PV/T) air heating collectors: steady-state simulation," *Renew. Energy*, Vol. 11, pp. 363–385. (1997).

Hegazy, A. A., "Comparative study of the performances of four photovoltaic / thermal solar air collectors," *Energy Convers. Manag.*, Vol. 41, pp. 861–881. (2000).

Holman, J., *Heat transfer*, Tata McGraw-Hill, (2010).

Joshi, A. S., Tiwari, A., Tiwari, G. N., Dincer, I. and Reddy, B. V., "Performance evaluation of a hybrid photovoltaic thermal (PV/T) (glass-to-glass) system," *Int. J. Therm. Sci.*, Vol. 48, pp. 154–164. (2009).

Kumar, R. and Rosen, M. A., "Performance evaluation of a double pass PV/T solar air heater with and without fins," *Appl. Therm. Eng.*, Vol. 31, pp. 1402–1410. (2011).

Kessaissia, F. Z., Zegaoui, A., Arab, A. H., Loukarfi, L. and Aillerie, M., "Comparison of Two PV Modules Technologies Using Analytical and Experimental Methods," *Energy Procedia*, Vol. 74, pp. 389–397. (2015).

Mohammadi, K. and Sabzpooshani, M., "Comprehensive performance evaluation and parametric studies of single pass solar air heater with fins and baffles attached over the absorber plate," *Energy*, Vol. 57, pp. 741–750. (2013).

Solanki, S. C., Dubey, S. and Tiwari, A., "Indoor simulation and testing of photovoltaic thermal (PV/T) air collectors," *Appl. Energy*, Vol. 86, pp. 2421–2428. (2009).

Sarhaddi, F., Farahat, S., Ajam, H. and Behzadmehr, A., "Exergetic performance assessment of a solar photovoltaic thermal (PV/T) air collector," *Energy Build.*, Vol. 42, pp. 2184–2199. (2010).

Tiwari, A. and Sodha, M. S., "Performance evaluation of solar PV/T system: An experimental validation," *Sol. Energy*, Vol. 80, pp. 751–759. (2006).

Teo, H. G., Lee, P. S. and Hawlader, M. N. A., "An active cooling system for photovoltaic modules," *Appl. Energy*, Vol. 90, pp. 309–315. (2012).

Watmuff, J. H., Charters, W. W. S. and Proctor, D., "Solar and wind induced external coefficients for solar collectors," *COMPLES*, Vol. 2, pp. 56. (1977).